THE JOURNAL OF PHYSICAL CHEMISTRY A LETTERS

2006, *110,* 5973−5977
Published on Web 04/18/2006

Resonance Raman Scattering of Rhodamine 6G as Calculated Using Time-Dependent Density Functional Theory

Lasse Jensen* and George C. Schatz

Department of Chemistry, Northwestern University, 2145 Sheridan Road, Evanston, Illinois 60208-3113

Received: February 20, 2006; In Final Form: March 27, 2006

In this work, we present the first calculation of the resonance Raman scattering (RRS) spectrum of rhodamine 6G (R6G) which is a prototype molecule in surface-enhanced Raman scattering (SERS). The calculation is done using a recently developed time-dependent density functional theory (TDDFT) method, which uses a short-time approximation to evaluate the Raman scattering cross section. The normal Raman spectrum calculated with this method is in good agreement with experimental results. The calculated RRS spectrum shows qualitative agreement with SERS results at a wavelength that corresponds to excitation of the S_1 state, but there are significant differences with the measured RRS spectrum at wavelengths that correspond to excitation of the vibronic sideband of S_1. Although the agreement with the experiments is not perfect, the results provide insight into the RRS spectrum of R6G at wavelengths close to the absorption maximum where experiments are hindered due to strong fluorescence. The calculated resonance enhancements are found to be on the order of 10^5. This indicates that a surface enhancement factor of about 10^{10} would be required in SERS in order to achieve single-molecule detection of R6G.

I. Introduction

Raman scattering of molecules absorbed on a rough metal surface can be enhanced by several orders of magnitude. This phenomenon is referred to as surface-enhanced Raman scattering (SERS) and was discovered some 30 years ago.[1−3] Recent progress in SERS has opened the possibility of using Raman techniques for ultrasensitive detection at the single molecule level.[4−7] The normal Raman scattering cross section of molecules is on the order of 10^{-30} cm^2/sr;[8] thus, the cross section has to be enhanced by a factor of $10^{14}-10^{15}$ if Raman spectroscopy is to be used for single molecule detection.

Such huge enhancements have been achieved using silver nanoparticle aggregates in conjunction with resonant enhancement due to a molecular electronic transition.[4−6] One such system where single molecule SERS has been observed is rhodamine 6G (R6G) absorbed on Ag nanoparticle aggregates.[4,5,7] R6G is a cationic dye with strong absorption in the visible and a high fluorescence yield. The molecule consists of two chromophores, a dibenzopyrene chomophore (xanthene), and a carboxyphenyl group tilted by about 90° with respect to the xanthene ring (see Figure 1). The π-systems of the two chromophores of R6G are therefore not conjugated. The strong absorption of R6G in aqueous solution has a maximum around 530 nm and a vibronic shoulder around 470 nm.[9]

When a R6G nanoparticle system is excited with visible light, it shows a molecular resonance Raman effect in addition to the SERS effect that comes from surface plasmon excitation. The combination of these effects leads to the large enhancements observed, and is often referred to as surface-enhanced resonance Raman scattering (SERRS). Furthermore, the strong fluorescence of R6G, which otherwise would prevent observation of the Raman spectrum, is quenched due to nonradiative interactions with the metal surface. For these reasons, many experimental SERS studies have been devoted to studies of R6G interacting with metal particles. Single molecule SERS experiments are done at wavelengths close to the absorption maximum of R6G, where the experimental resonance Raman scattering (RRS) spectrum cannot be obtained due to the strong fluorescence. Therefore, little is known about the RRS spectrum at wavelengths close to the absorption maximum. A few studies have focused on the relative importance of resonance enhancement versus surface enhancement at 530 nm, but the absence of an RRS spectrum has been a hindrance. It is, however,

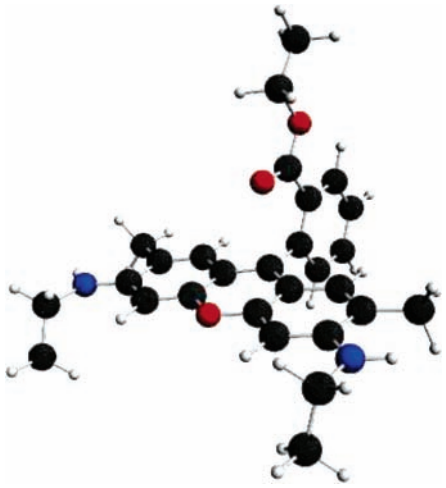

Figure 1. Structure of Rhodamine 6G.

* Electronic address: l.jensen@chem.northwestern.edu.

10.1021/jp0610867 CCC: $33.50

expected that surface enhancement is the dominant contribution, since resonance enhancement is generally on the order of 10^4–10^6.[8]

In this work, we will address these issues by calculating the normal Raman scattering (NRS) and RRS spectra of R6G, with the RRS result referring to a wavelength corresponding to its absorption maximum. The calculations will be done using a recently developed time-dependent density functional theory (TDDFT) method, which uses a short-time approximation to evaluate the Raman scattering cross section.[10,11] This short-time approximation makes it possible to calculate both NRS and RRS intensities from the geometrical derivatives of the frequency-dependent polarizability. Therefore, we will not only get information about the RRS spectrum but also the absolute intensities and thereby an estimate of the magnitude of the resonance enhancement.

II. Computational Details

All calculations presented in this work have been done using a local version of the Amsterdam Density Functional (ADF) program package.[12,13] The Becke–Perdew (BP86) XC potential[14,15] and a triple-ζ polarized Slater-type (TZP) basis set from the ADF basis set library have been used. The vibrational frequencies and normal modes were calculated within the harmonic approximation. For this reason, the BP86 functional has been chosen since it usually gives harmonic frequencies close to experimental results without the use of scaling factors.[16] We have also successfully used this functional and basis set in earlier studies of RRS spectra for simpler, but chemically similar, molecules.[11] Full geometry optimization, excitation energies, and frequency calculations have been performed prior to the polarizability calculations. The polarizability derivatives are then calculated by numerical three-point differentiation with respect to the normal mode displacements as described in detail in ref 17. This allows us to selectively study the Raman intensities of the normal modes associated with the frequency range between 500 and 1800 cm^{-1}. The electronic polarizability both on and off resonance is calculated by including the finite lifetime of the electronic excited states in the TDDFT calculation.[10,11] The finite lifetime is included phenomenologically using a common damping parameter $\Gamma \approx 0.004$ au (800 cm^{-1}), which is what we have found previously to be reasonable for other molecules.[10,11]

Absolute Raman intensities are presented here as the differential Raman scattering cross section. For Stokes scattering with an experimental setup having a 90° scattering angle and perpendicular plane-polarized light, the cross section is given by[18]

$$\frac{d\sigma}{d\Omega} = \frac{\pi^2}{\epsilon_0^2}(\tilde{\nu}_{in} - \tilde{\nu}_p)^4 \frac{h}{8\pi^2 c\tilde{\nu}_p}[45\bar{\alpha}_p'^2 + 7\gamma_p'^2]\frac{1}{45[1 - \exp(-hc\tilde{\nu}_p/k_B T)]} \quad (1)$$

where $\tilde{\nu}_{in}$ and $\tilde{\nu}_p$ are the frequencies of the incident light and of the pth vibrational mode, respectively. $\bar{\alpha}_p'$ and γ_p' are the isotropic and anisotropic polarizability derivatives with respect to vibrational mode p.

III. Results and Discussion

Recently, Watanabe et al.[19] calculated the NRS spectrum of R6G using the B3LYP functional in order to analyze experimental spectra obtained using various Raman techniques, in particular, Tip-enhanced Raman spectroscopy. Comparing the spectrum obtained here using the BP86 functional with the spectrum from B3LYP, we find in general quite good agreement with respect to both the frequencies and the relative intensities. The vibrational frequencies from these two functionals agree to within 10 cm^{-1}, although they reported scaled frequencies, whereas we report unscaled values.

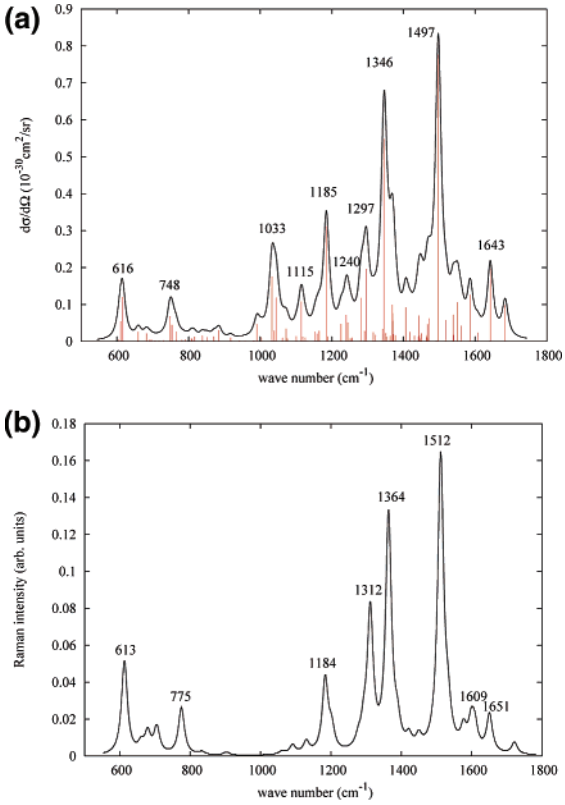

Figure 2. NRS spectrum for R6G. (a) Differential cross section of R6G in units of 10^{-30} cm^2/sr at an incident wavelength of 1064 nm, calculated using a damping of $\Gamma = 0.004$ au. The spectrum has been broadened with a Lorentzian having a width of 20 cm^{-1}. (b) Relative intensities constructed from experimental data reported in Table 3 of ref 19 and broadened with a Lorentzian having a width of 20 cm^{-1}.

The experimental NRS spectrum is obtained in ethanol solution using an incident wavelength of 1064 nm.[19] The BP86 simulated spectrum and the experimental NRS spectrum are presented in Figure 2 in the frequency range between 500 and 1800 cm^{-1}. The polarizability derivatives needed in eq 1 were calculated from the static polarizability; however, a wavelength of 1064 nm was assumed for calculations of the differential cross section. The experimental spectrum is constructed from the intensity data reported in Table 3 of ref 19 and broadened with a Lorentzian having a width of 20 cm^{-1} in order to compare with the results presented here. From Figure 2, we see that the simulated spectrum is in quite good agreement with the experimental spectrum, even though solvent effects and anharmonic corrections are ignored in the calculation. A collection of important bands together with their assignments are presented in Table 1. The vibrational motion of a molecule the size of R6G is quite complicated, and the assignments given are based on the major contributions. In general, the assignments are in good agreement with earlier results,[9,19,20] except that we do not assign the two peaks at 775 and 613 cm^{-1}, since there are several modes in these regions having significant intensities. In SERS experiments,[9,21] it has been observed that the peak at 775 cm^{-1} under certain conditions splits into two peaks around 776 and 766 cm^{-1}, which is in agreement with the results presented here.

In the measured NRS spectrum, the two strongest bands correspond to the aromatic C−C stretch modes at 1512 and 1364 cm^{-1}. This is in good agreement with the BP86 results with respect to both peak position (within 20 cm^{-1}) and relative intensity of the two bands. The major difference between the experimental and simulated spectra is nearly 1033 cm^{-1}. This region of the experimental spectrum shows only very weak peaks, whereas in the simulated spectrum, two bands are found. The bands in this region of the spectrum correspond mainly to motion in the amino ethyl group. The reason that these bands are not seen in the experimental spectrum is because the solvent (ethanol) has Raman bands in the same region and the solvent background has been removed.[22]

Before we proceed to the RRS spectrum of R6G, we need to characterize the $S_0 \rightarrow S_1$ transition. The lowest excitation energy is found to be 2.62 eV (474 nm), with an oscillator strength of 0.6 using the BP86 functional. This $S_0 \rightarrow S_1$ transition corresponds to a highest occupied molecular orbital (HOMO) to lowest unoccupied molecule orbital (LUMO) transition. Experimentally, it is found that the strong absorption of R6G in aqueous solution has a maximum around 530 nm (2.33 eV) with a vibronic shoulder at around 470 nm.[9] Since we do not consider vibronic coupling effects, modeling of the shoulder cannot be done. The calculated maximum is about 0.3 eV higher than the experimental result. Since the experiment is done in aqueous solution, solvent effects are a likely explanation for the difference. To test this, we calculated the excitation energies in solution by means of the conductor-like screening model of solvation (COSMO).[23−25] The excitation energy in aqueous solution was found to be 2.44 eV (508 nm), which is in much better agreement with the experimental result. Therefore, most of the differences in the excitation energy between theory and experiment can be ascribed to solvent effects. Although solvent effects are likely to also be important for the Raman spectrum, we will not consider this type of calculation further due to the much larger computational burden. Also, the NRS spectrum was described reasonably well without the inclusion of solvent effects, so it will be interesting to see how well this works for the RRS spectrum. The orbitals involved in the $S_0 \rightarrow S_1$ transition are presented in Figure 3. It is clear to see that both the HOMO and the LUMO are localized in the xanthene chromophore and the nitrogen of the ethylamino group. Therefore, one would expect vibrations which involve motion of the xanthene ring of R6G to be strongly resonance enhanced by a transition to the S_1 state.

Having shown that the adopted method provides a good description of the NRS spectrum of R6G, we will proceed to the RRS spectrum for which little is known from a theoretical point of view. We are particularly interested in the RRS spectrum at the absorption maximum and the resonance enhancement associated with it. However, as mentioned earlier, it is not possible experimentally to obtain the RRS spectrum of R6G at a wavelength of 530 nm due to strong fluorescence. As a result, the experimental RRS spectrum[9,19] is obtained choosing a wavelength close to the vibrational shoulder. Since RRS spectroscopy probes the excited-state dynamics, even small changes in excitation wavelength can have a large effect on the RRS spectrum, especially if the absorption spectrum shows vibronic structure.[26] This is clear if one compares the RRS spectrum obtained by Hildebrandt and Stockburger[9] at 457 nm with the spectrum at 488 nm obtained by Watanabe et al.[9] While the SERS spectrum is available for wavelengths close to the absorption maximum, a direct comparison of this to the RRS spectrum is hindered by possible interaction with the silver surface. Another issue that complicates the comparison between theory and experiment is that the short-time approximation to the Raman scattering might not provide a complete description, especially given that the experimental absorption spectrum shows vibrational structure. However, we have shown that a short-time approximation can be useful even for these difficult situations.[11] Thus, to provide a complete picture, we will compare the calculated RRS spectrum at the absorption maximum with two experimental spectra, the RRS result (in ethanol) of Watanabe et al.[19] at 488 nm and the SERS spectrum of Brus and co-workers[7] at 514.5 nm.

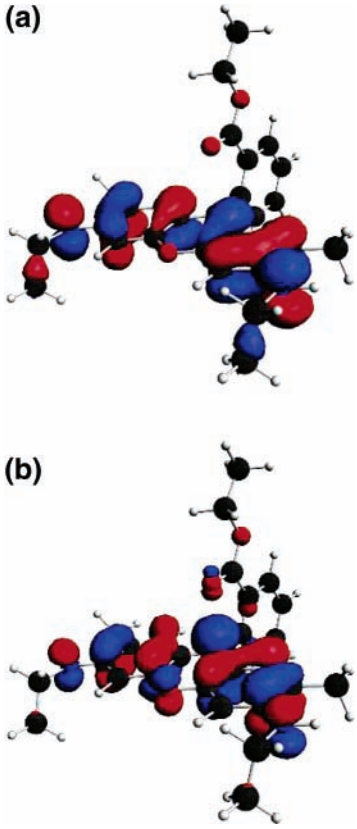

Figure 3. The HOMO (a) and LUMO (b) of R6G involved in $S_0 \rightarrow S_1$ transition.

For excitation to the S_1 state (our excitation wavelength 474 nm), the calculated RRS spectrum of R6G is presented in Figure 4 along with the two experimental spectra just mentioned. The Watanable et al. spectrum is constructed from the data reported in Table 3 of ref 19. As expected, this spectrum shows important differences with the calculated results. The most noticeable difference is for the two peaks at 611 and 775 cm^{-1}, which in the experimental spectrum are very strong whereas they are relatively weak in the simulated spectrum. As mentioned earlier, the wavelength used in the experiment is 488 nm, which corresponds to an excitation into the vibronic shoulder around 470 nm.[9] It is therefore quite likely that these two bands gain some of their enhancement by a vibronic coupling mechanism.[8] This was also suggested in the earlier experimental work of Hildebrandt and Stockburger,[9] since no overtones were found for these bands. Our results seem to support this conclusion. In single-molecule SERS experiments,[27] it has been noted that the two bands around 611 and 775 cm^{-1} show particularly large fluctuations. This, however, was explained in terms of charge-transfer excitations between the silver and the R6G. Our results indicate that a vibronic coupling mechanism might also contribute to the observed fluctuations.

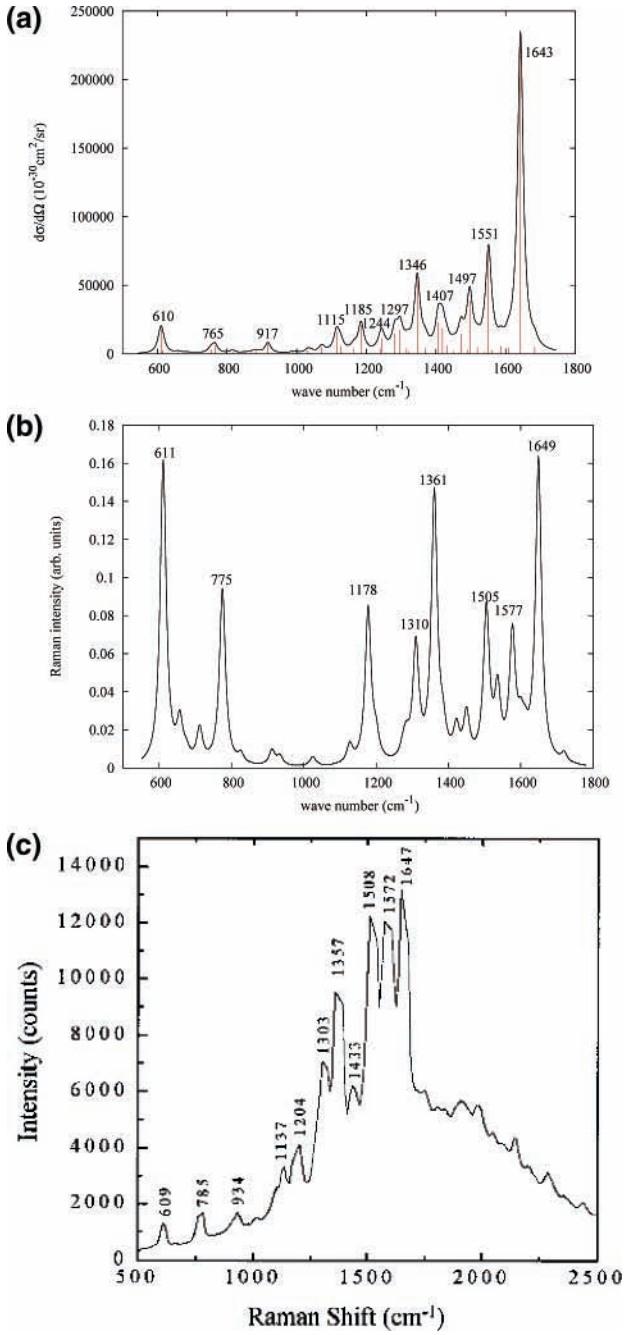

Figure 4. RRS spectrum of R6G. (a) Differential cross section for the S_1 state of R6G in units of 10^{-30} cm^2/sr at an incident wavelength of 474 nm. Calculated using a damping of $\Gamma = 0.004$ au. Spectrum has been broadened with a Lorentzian having a width of 20 cm^{-1}. (b) Relative intensities constructed from the data reported in Table 3 of ref 19 and broadened with a Lorentzian having a width of 20 cm^{-1}. (c) SERS spectrum taken from ref 7.

Other bands which show strong resonance enhancements correspond to C−C stretching in the xanthene plane and are found at 1649, 1577, 1505, and 1361 cm^{-1}. Since all of these bands involve some character of xanthene in-plane C−C stretching, they are expected to show resonance enhancements. These bands are also found to be strongly enhanced in the simulated RRS spectrum; in particular, the band at 1649 cm^{-1} is very strong. The band at 1577 cm^{-1} was previously assigned by Watanabe[19] to a symmetric C−C stretching in the phenyl ring. However, we do not find this mode to be resonance-enhanced.

TABLE 1: Assignment and Resonance Enhancement Factors (EF) of Selected Bands of R6G[a]

exp. NRS	exp. RRS	BP86	assignment	EF
613	611	610	ip XRD	1.4×10^6
613	611	616	op XRD	9.2×10^4
775	775	748	op C−H bend	1.3×10^4
775	775	754	op C−H bend	3.0×10^5
775	775	765	ip XRD	1.0×10^6
1184	1178	1185	ip XRD, C−H bend, N−H bend	2.8×10^5
1312	1310	1297	ip XRB N−H bend, CH2 wag	3.7×10^5
1364	1361	1346	XRS, ip C−H bend	4.1×10^5
1512	1505	1497	XRS, C−N str, C−H bend, N−H bend	2.1×10^5
1577	1577	1551	XRS, ip N−H bend	2.8×10^6
1651	1649	1643	XRS, ip C−H bend	4.9×10^6

[a] ip: in plane. op: out of plane. XRD: xanthene ring deformations. XRB: xanthene ring breath. XRS: xanthene ring stretch. str: stretch.

We find much better agreement between our simulated RRS spectrum and the experimental SERS spectrum. The biggest differences between the experimental SERS and RRS spectra is for the two bands around 611 and 775 cm^{-1}. In the SERS spectrum, these bands are much weaker compared with the C−C stretch bands in the 1500−1650 cm^{-1} region. This is in good agreement with our simulated spectrum. In general, there is good agreement between theory and the SERS experiment on which mode shows resonance enhancement, although the band at 1643 cm^{-1} in the simulated spectrum is much stronger than in the experiment. This agreement between calculated and SERS spectra is encouraging, and it suggests that the previously unobserved RRS spectrum at 530 nm should be closer to the SERS spectrum than to the RRS spectrum at 488 nm. Interactions with the surface will, of course, have some effect, but past studies of other molecules suggest that these effects can be of secondary importance.[2]

If we consider the absolute intensities of the simulated RRS spectrum, we see that they are on the order of 10^{-25} cm^2/sr, which corresponds to a resonance enhancement of 10^5−10^6. The specific enhancements for different modes are collected in Table 1. The enhancements are calculated as the ratio of the RRS and the NRS differential cross sections. As expected, we see that the modes involving in-plane motion in the xanthene chromophore are enhanced more than other modes. This means that in order to obtain Raman cross sections for R6G which are in the single-molecule limit an additional surface enhancement of roughly 10^{10} is required. This is in good agreement with a recent model study,[28,29] which showed that a resonant Raman cross section of $\sim 10^{-14}$ cm^2/sr (for isolated R6G of $\sim 10^{-24}$ cm^2/sr) can be achieved by a surface enhancement of around 10^{10}. Such large surface enhancements are in agreement with predictions from electrodynamics calculations for the strong local field found in nanoparticle junctions.[30]

Conclusions

In this work, the first calculation of the RRS spectrum of the SERS prototype molecule, R6G, for the S_1 state is presented. The results provide insights into the RRS spectrum of R6G at frequencies close to the absorption maximum which is not accessible from experiments due to strong fluorescence. We find the simulated NRS spectrum to be in good agreement with experimental results even though solvent effects and anharmonic corrections are not included in the calculations. For the RRS spectrum, there are significant differences between the relative intensities obtained from an RRS experiment at a shorter wavelength and that calculated theoretically. This is particularly

clear for the two bands found around 611 and 775 cm^{-1}, and it is therefore likely that they gain some of their intensity from vibronic coupling. Better agreement is found for the calculated RRS spectrum and that obtained from SERS measurements at the absorption maximum. The calculated resonance enhancements are found to be on the order of 10^5. This indicates that about a factor of 10^{10} is required in SERS in order to achieve single-molecule detection of R6G. Such surface enhancements are in good agreement with the strong local field found in nanoparticle junctions.

Acknowledgment. L.J. and G.C.S. thank the Air Force Office of Scientific Research MURI program (F49620-02-1-0381). This research was performed in part using the Molecular Science Computing Facility (MSCF) in the William R. Wiley Environmental Molecular Sciences Laboratory, a national scientific user facility sponsored by the U.S. Department of Energy's Office of Biological and Environmental Research and located at the Pacific Northwest National Laboratory, operated for the Department of Energy by Battelle.

References and Notes

(1) Fleischman, M.; Hendra, P. J.; McQuillan, A. *J. Chem. Phys. Lett.* **1974**, *26*, 163−166.
(2) Jeanmaire, D. L.; Van Duyne, R. P. *J. Electroanal. Chem.* **1974**, *84*, 1−20.
(3) Albrecht, M. G.; Crieghton, J. A. *J. Am. Chem. Soc.* **1977**, *99*, 5215−5217.
(4) Nie, S. M.; Emory, S. R. *Science* **1997**, *275*, 1102−1106.
(5) Kneipp, K.; Wang, Y.; Kneipp, H.; Perelman, L. T.; Itzkan, I.; Dasari, R. R.; Feld, M. S. *Phys. Rev. Lett.* **1997**, *78*, 1667−1670.
(6) Xu, H.; Bjerneld, E. J.; Käll, M.; Börjesson, L. *Phys. Rev. Lett.* **1999**, *83*, 4357−4360.
(7) Michaels, A. M.; Nirmal, M.; Brus, L. E. *J. Am. Chem. Soc.* **1999**, *121*, 9932−9939.
(8) Asher, S. A. *Annu. Rev. Phys. Chem.* **1988**, *39*, 537−588.
(9) Hildebrandt, P.; Stockburger, M. *J. Phys. Chem.* **1984**, *88*, 5935−5944.
(10) Jensen, L.; Autschbach, J.; Schatz, G. C. *J. Chem. Phys.* **2005**, *122*, 224115.
(11) Jensen, L.; Zhao, L.; Autschbach, J.; Schatz, G. C. *J. Chem. Phys.* **2005**, *123*, 174110.
(12) ADF; http://www.scm.com, 2005.
(13) te Velde, G.; Bickelhaupt, F. M.; Baerends, E. J.; Fonseca Guerra, C.; van Gisbergen, S. J. A.; Snijders, J. G.; Ziegler, T. *J. Comput. Chem.* **2001**, *22*, 931.
(14) Becke, A. D. *Phys. Rev. A* **1988**, *38*, 3098.
(15) Perdew, J. P. *Phys. Rev. B* **1986**, *33*, 8822.
(16) Neugebauer, J.; Hess, B. A. *J. Chem. Phys.* **2003**, *118*, 7215−7225.
(17) Reiher, M.; Neugebauer, J.; Hess, B. A. Z. *Phys. Chem.* **2003**, *217*, 91−103.
(18) Neugebauer, J.; Reiher, M.; Kind, C.; Hess, B. A. *J. Comput. Chem.* **2002**, *23*, 895−910.
(19) Watanabe, H.; Hayazawa, N.; Inouye, Y.; Kawata, S. *J. Phys. Chem. B* **2005**, *109*, 5012−5020.
(20) Majoube, M.; Henry, M. *Spectrochim. Acta* **1991**, *47A*, 1459−1466.
(21) Vosgröne, T.; Meixner, A. J. *ChemPhysChem* **2005**, *6*, 154−163.
(22) Hildebrandt, P.; Keller, S.; Hoffman, A.; Vanhecke, F.; Schrader, B. *J. Raman Spectrosc.* **1993**, *24*, 791−796.
(23) Klamt, A.; Schüürmann, G. *J. Chem. Soc., Perkin Trans. 2* **1993**, 799−805.
(24) Pye, C. C.; Ziegler, T. *Theor. Chim. Acta* **1999**, *101*, 396−407.
(25) The COSMO calculations were done using a recently developed extension of the existing implementation within ADF. This new code now includes the dynamic response of the solvent due to the perturbing electric field, which was missing previously. Also, nonequilibrium solvation response is implemented, which is important for calculation of the response properties. The static and optical dielectric constants for water were taken to be 78.5 and 1.777, respectively, in these calculations.
(26) Jones, C. M.; Asher, S. A. *J. Chem. Phys.* **1988**, *89*, 2649−2661.
(27) Weiss, A.; Haran, G. *J. Phys. Chem. B* **2001**, *105*, 12348−12354.
(28) Xu, H.; Wang, X.-H.; Persson, M. P.; Xu, H. Q.; Käll, M.; Johansson, P. *Phys. Rev. Lett.* **2004**, *93*, 243002.
(29) Johansson, P.; Xu, H.; Käll, M. *Phys. Rev. B* **2005**, *72*, 035427.
(30) Hao, E.; Schatz, G. C. *J. Chem. Phys.* **2004**, *120*, 357.